Research Article

Journal of PeptideScience

Received: 5 July 2010 Revised: 5 October 2010 Accepted: 6 October 2010 Published online in Wiley Online Library: 4 February 2011

(wileyonlinelibrary.com) DOI 10.1002/psc.1323

Desirability function combining metabolic stability and functionality of peptides‡

Sylvia Van Dorpe,[a§] Antita Adriaens,[b§] Simon Vermeire,[c] Ingeborgh Polis,[b] Kathelijne Peremans[c] and Bart De Spiegeleer[a*]

The evaluation of peptides as potential therapeutic or diagnostic agents requires the consideration of several criteria that are targeted around two axes: functionality and metabolic stability. Most often, a compromise has to be made between these mutually opposing characteristics.

In this study, Derringer's desirability function, a multi-criteria decision-making method, was applied to determine the best peptide for opioid studies in a single figure-of-merit.

The penetration of the blood–brain barrier (BBB) determines the biological functionality of neuropeptides in the brain target tissue, and consists of an influx and an efflux component. The metabolic stability in the two concerned tissues, i.e. plasma and brain, are taken into consideration as well. The overall selection of the peptide drug candidate having the highest BBB-drugability is difficult due to these conflicting responses as well as the different scalings of the four biological parameters under consideration.

The highest desirability, representing the best BBB-drugability, was observed for dermorphin. This peptide is thus the most promising drug candidate from the set of eight opioid peptides that were investigated. The least desirable candidate, with the worst BBB influx and/or metabolic stability, was found to be CTAP. Validation of the desirability function by *in vivo* medical imaging showed that dermorphin and DAMGO penetrate the BBB, whereas EM-1 and TAPP did not. These results are thus consistent with those obtained with the desirability evaluation.

To conclude, the multi-criteria decision method was proven to be useful in biomedical research, where a selection of the best candidate based on opposing characteristics is often required.

Supporting information may be found in the online version of this article

Keywords: Blood–brain barrier; desirability; metabolic stability; μ-opioid receptor peptides; SPECT medical imaging

Introduction

To determine the possible drugability of a peptide, the functionality needs to be evaluated. Well-known and typical functionality investigations include receptor binding assays, cell and tissue studies, penetration of biological barriers and tissue distribution and uptake. In radioligand binding studies, receptor affinity or selectivity is studied to characterize the receptors or ligands pharmacologically [1–8]. Studies involving the penetration of biological barriers are often focused on the transport of drugs through the blood–brain barrier (BBB). Transport through the BBB is essential to target brain receptors with possible application in the diagnosis or treatment of central nervous system (CNS) diseases [9–12]. The BBB separates blood from brain and strictly regulates the influx of compounds due to the presence of tight junctions and selective influx/efflux-systems [13,14]. This way, the optimal conditions for neuronal function are maintained, while harmful compounds are prevented from entering the brain. The CNS peptides constitute an important peptide group with pharmaceutical potential provided they can penetrate the BBB in order to exert their action. The critical functionality of neuropeptide drugs thus consists of the BBB influx as well as efflux. These two biological parameters are commonly estimated from *in vivo* mouse experiments upon intravenous or intracerebral injection [15,16].

Another critical aspect is the duration that peptides are presented to the brain, which is *inter alia* determined by the stability in plasma and brain tissue. Therefore, the metabolic stability in these two tissues should be determined as well. One of the major bottlenecks in the development of peptide drugs is their

* *Correspondence to: Bart De Spiegeleer, Drug Quality and Registration (DruQuaR) Group, Faculty of Pharmaceutical Sciences, Ghent University, Harelbekestraat 72, B-9000 Ghent, Belgium. E-mail: Bart.DeSpiegeleer@UGent.be*

a *Drug Quality and Registration (DruQuaR) Group, Faculty of Pharmaceutical Sciences, Ghent University, Harelbekestraat 72, B-9000 Ghent, Belgium*

b *Department of Medicine and Clinical Biology of Small Animals, Faculty of Veterinary Medicine, Ghent University, Salisburylaan 133, B-9820 Merelbeke, Belgium*

c *Department of Veterinary Medical Imaging and Small Animal Orthopaedics, Faculty of Veterinary Medicine, Ghent University, Salisburylaan 133, B-9820 Merelbeke, Belgium*

‡ *Special issue devoted to contributions presented at the 12th Naples Worshop on Bioactive Peptides and 2nd Italy-Korea Symposium on Antimicrobial Peptides, 4–7 June 2010, Naples, Italy.*

§ *These authors contributed equally to this work.*

Journal of PeptideScience

Table 1. Opioid peptides information

Peptide	Sequence[a]	Receptor action	Origin	Analog of
CTAP	fCYwRT-Pen-T–NH_2[b]	Antagonist	Synthetic	Somatostatin
CTOP	fCYw-Orn-T-Pen-T–NH_2[b,c]	Antagonist	Synthetic	Somatostatin
EM-1	YPWF–NH_2	Agonist	Endogenous	–
EM-2	YPFF–NH_2	Agonist	Endogenous	–
TAPP	YaFF–NH_2	Agonist	Synthetic	EM-2
TAPS	YrF-Sar[d]	Agonist	Synthetic	Dermorphin
Dermorphin	YaFGYPS–NH_2	Agonist	Biologic (frog skin)	–
DAMGO	YaGF(Me)G–OH[e]	Agonist	Synthetic	Enkephalin

[a] Amino acids written in small letters represent D-amino acid residues.
[b] Pen = penicillamine; disulfide bridge between C and Pen.
[c] Orn = ornithine; disulfide bridge between C and Pen.
[d] Sar = sarcosine.
[e] F(Me) = methylated phenylalanine; G–OH represents the hydroxylated form of glycine.

sensitivity to enzymatic degradation [17]. Although it is described that some endogenous peptide drugs are less susceptible to enzymatic degradation due to their unique structure [18], most peptide drugs are chemically modified to enhance their metabolic stability [3,19–25]. For the correct decision of the 'best peptide', it is therefore required to investigate and take into account the metabolic stability as well. This metabolic fate of compounds is mostly tested *in vitro* by incubation in, e.g. plasma and organ homogenates [21,22,26,27].

These two aspects (functional BBB transport and metabolic stability) were previously investigated using eight μ-opioid receptor (MOR) peptides that have been shown to demonstrate a high affinity and selectivity for the MOR and that constitute a group of possible peptide drugs in pain treatment (agonist) or addiction treatment (antagonist) [28]. In order to select the best peptide for biomedical research, we have now combined the four biological responses (BBB influx and efflux as well as metabolic stability in brain and plasma) using a multi-criteria decision method. This approach enables us to simultaneously evaluate these four responses that have different scalings by transforming them into a dimensionless desirability scale, which results in a single figure-of-merit [29,30]. The desirability approach is an important tool in selecting the optimum peptide objectively and quantitatively, with 'optimum' being defined as the best compromise between BBB transport and metabolic stability characteristics, i.e. the peptide with the highest BBB-drugability. Although this approach is quite frequently applied in other fields like chromatographic analysis [31], such multi-criteria decision methods have found much less acceptance in biomedical research [32].

The obtained global desirability function was then validated by *in vivo* imaging using single photon emission computed tomography (SPECT).

Materials and Methods

Animals

Male mice from the Institute for Cancer Research, Caesarean Derived-1 (ICR-CD-1) (Harlan Laboratories, Venray, The Netherlands), weighing 25–30 g, were used according to the Ethical Committee principles of laboratory animal welfare as approved by our institute (Ghent University, Faculty of Veterinary Medicine, 2009-065). Mouse plasma was obtained from Harlan Laboratories as well.

Peptides

The eight opioid peptides, shown in Table 1, were synthesized by Peptide Protein Research (PPR, Hampshire, United Kingdom) with a purity of at least 95%. Quality control data are given in Supporting Information. The impurity profile was examined using HPLC–UV/MS as previously reported [33].

Reagents

Calcium chloride hydrate and Krebs–Henseleit buffer were purchased from Sigma (St. Louis, MO, USA). Disodium hydrogen phosphate dihydrate, sodium dihydrogen phosphate monohydrate and sodium iodide were obtained from Merck KGaA (Darmstadt, Germany). Sodium bicarbonate was purchased from UCB (Brussels, Belgium) and 99+% formic acid from Acros Organics (Geel, Belgium). $Na^{123}I$ was supplied by GE Healthcare (Waver, Belgium).

Peptide Lyophilization

Prior to experimental use, the opioid peptides were dissolved in a mixture of acetonitrile and 0.1% w/v aqueous formic acid (5/95 v/v) at a concentration of 1 mg/ml. The peptide solutions were then dispensed into microtubes and lyophilized using a Gamma 1–16 LSC shelf freeze-dryer (Martin Christ, Osterode am Harz, Germany).

Quantitative Multi-criteria Evaluation: Desirability Function

We previously reported the BBB influx transport of eight opioid peptides by multiple-time regression and capillary depletion as well as efflux transport. Additionally, the *in vitro* metabolic stability in mouse plasma and brain homogenate was obtained [28]. Owing to the large difference in metabolization constants, the logarithm was calculated as well as the standard errors on the regression coefficients (Table 2). The standard error on the logarithm transformation was calculated using the following error propagation rule:

$$s_x = 0.434\frac{s_a}{a} \text{ [34]} \quad (1)$$

In order to optimize these four different responses, which have different scalings, the use of a multi-criteria decision technique was required. Therefore, the responses were transformed into

Table 2. BBB transport properties and *in vitro* metabolic stability

Peptide	K_{in} (µl/(g×min))	k_{out} (min^{-1})	log (k_{brain})	log (k_{plasma})
Dermorphin	2.18 ± 1.78	0.000 ± 0.032	0.795 ± 0.034	1.083 ± 0.031
DAMGO	0.40 ± 0.55	0.065 ± 0.024	0.380 ± 0.023	1.418 ± 0.028
TAPP	1.12 ± 0.62	0.25 ± 0.093	0.867 ± 0.022	1.158 ± 0.048
CTOP	0.24 ± 0.44	0.000 ± 0.092	0.665 ± 0.027	1.255 ± 0.049
TAPS	0.18 ± 0.45	0.000 ± 0.041	0.581 ± 0.034	0.943 ± 0.041
EM-1	1.06 ± 0.58	0.047 ± 0.061	1.529 ± 0.14	3.009 ± 0.014
EM-2	1.14 ± 0.75	0.032 ± 0.019	1.896 ± 0.040	3.279 ± 0.16
CTAP	0.00 ± 0.25	0.000 ± 0.038	1.767 ± 0.15	2.061 ± 0.066

a dimensionless desirability (d) scale via the following linear desirability function:

$$d(Y) = \frac{Y_i - 0.9Y_{min}}{1.1Y_{max} - 0.9Y_{min}} \text{ or } d(Y) = \frac{1.1Y_{max} - Y_i}{1.1Y_{max} - 0.9Y_{min}} \quad (2)$$

for parameters to be maximized (K_{in}) or minimized (k_{out}, log k_{brain} and log k_{plasma}), respectively.

In these equations, Y_i was the experimental value for the respective response, whereas Y_{min} and Y_{max} were the minimum and maximum acceptable response values, respectively.

The obtained linear transformation d(Y) ranges from nearly 0 (undesirable) to nearly 1 (most desirable). As a result, values of the different properties, which have a different range scaling, can be combined. Finally, from these *d*-values, a global *D*-value was calculated as the geometric mean [30]:

$$D = \sqrt[n]{\prod_{i=1}^{n} d_i^{p_i}} \quad (3)$$

In this equation, p_i was the relative importance assigned to the response. In this evaluation, we used $p_i = 1$ for each of the four responses. In this study, n equals 4 since four characteristics were considered in the global evaluation. The peptide with the highest *D*-value expresses the best combination of the different responses and thus the highest overall BBB-drugability. The advantage of calculating the geometric mean is that when one of the criteria has an unacceptable value, the overall product will be unacceptable as well. This Derringer's desirability function was first introduced in chromatography by Deming [29,34]. In biomedical research, however, the Derringer approach has hardly been applied before [32,36].

In vivo Imaging

Before starting the *in vivo* SPECT imaging analysis, the peptides (dermorphin, DAMGO, EM-1 and TAPP) were radiolabeled with I-123 using the Iodogen method. Briefly, 100 µg of the peptide was dissolved in 100 µl of phosphate buffer (130 mM, pH 7.4). An Iodo-Gen® coated tube was previously rinsed with 1 ml phosphate buffer. Subsequently, 50 µl phosphate buffer and 1 µl of $Na^{123}I$ solution (37 MBq/µl; theoretical specific activity of 4.25 pmole) were transferred into this Iodo-Gen® coated tube. After 6 min at room temperature, the oxidation reaction of iodide to iodonium was stopped by removing the solution from the tube and adding the obtained iodonium solution to a tube containing 50 µl of peptide solution. The iodination reaction of the peptide was allowed to proceed for another 6 min at room temperature. After labeling, the mono-iodinated peptide was isolated on a Vydac Everest C_{18} (250 mm length × 4.6 mm internal diameter, 300 Å, 5 µm particle size) HPLC column (Grace Vydac, Hesperia, CA, USA) in an oven set at 30 °C, with a mobile phase consisting of (A) 0.1% w/v formic acid in water and (B) 0.1% w/v formic acid in acetonitrile. For each peptide, a different linear gradient was employed as follows:

1. Dermorphin and EM-1: 0–30 min going from 95% A to 70% A
2. DAMGO: 0–30 min going from 95% A to 75% A
3. TAPP: 0–30 min going from 95% A to 60% A

This was followed by reconditioning with the initial composition for 15 min. In each method, the flow rate was set at 1.0 ml/min and the injection volume was 100 µl.

The radio-HPLC apparatus consisted of a LaChrom Elite L-2130 pump with degasser, a LaChrom Elite L-2300 column oven, a LaChrom Elite L-2400 UV detector set at 215 nm (all Hitachi, Tokyo, Japan), a Rheodyne 7725i manual injector with 100 µl sample loop (Rheodyne, Rohnert Park, CA, USA) and a Berthold LB500 HERM radioactivity detector (Berthold Technologies, Bad Wildbad, Germany) equipped with EZChrom Elite version 3.1.7 software for data acquisition (Scientific Software, Pleasanton, CA, USA). After HPLC purification, the solvent was evaporated under N_2 gas flow at room temperature, the peptide was reconstituted in phosphate buffer and the radioactivity of an aliquot was measured using a dose calibrator.

Finally, anesthesia in mice was induced with isoflurane (Isolflo, Abbott Laboratories) in oxygen (4–5%) after which 200 µl of the I-123 labeled peptide was injected intravenously in the tail vein of the mouse. Acquisition was performed under general anesthesia (1.5–2% isoflurane in oxygen) using a triple head gamma camera (Triad, Trionix, Twinsburg, OH, USA) equipped with Low Energy Ultrahigh Resolution (LEUHR) parallel hole collimators. The acquisition matrix was 128 × 128. Scanning was initiated directly after the injection of the I-123 peptide tracer and dynamic acquisitions were performed for 3 h: 10 frames of 60 s and 34 frames of 300 s. The acquired images were processed with Gold software version 2.10 (Nuclear Diagnostics AB, Stockholm, Sweden) for dynamic studies. Region of interest (ROI) analysis was performed on the obtained images. ROIs were manually drawn on the composite image and included: (i) thyroid, (ii) heart, (iii) stomach, (iv) bladder, (v) brain, (vi) intestines and (vii) background. Since two different time frames (1 and 5 min) were used, the data of the initial time frames was added to 5 min in order to obtain equal time frames. The radioactivity was corrected for the injected dose, as this differed between the animals. Finally, a radioactivity curve was obtained representing the corrected radioactivity *versus* time. As

Journal of PeptideScience

Table 3. Individual and global desirability values

Peptide	$d(K_{in})$	$d(k_{out})$	$d(\log k_{brain})$	$d(\log k_{plasma})$	D
Dermorphin	0.826 ± 0.674	1.000	0.743 ± 0.034	0.888 ± 0.030	0.859
DAMGO	0.152 ± 0.208	0.803 ± 0.297	0.946 ± 0.023	0.784 ± 0.028	0.548 ± 0.195
TAPP	0.424 ± 0.235	0.242 ± 0.090	0.707 ± 0.022	0.865 ± 0.048	0.501 ± 0.084
CTOP	0.091 ± 0.167	1.000	0.807 ± 0.027	0.835 ± 0.049	0.497
TAPS	0.068 ± 0.170	1.000	0.848 ± 0.034	0.931 ± 0.041	0.482
EM-1	0.402 ± 0.220	0.858 ± 1.113	0.383 ± 0.135	0.294 ± 0.014	0.444 ± 0.156
EM-2	0.432 ± 0.284	0.903 ± 0.536	0.203 ± 0.040	0.210 ± 0.159	0.359 ± 0.080
CTAP	0.000	1.000	0.266 ± 0.153	0.586 ± 0.067	0.000

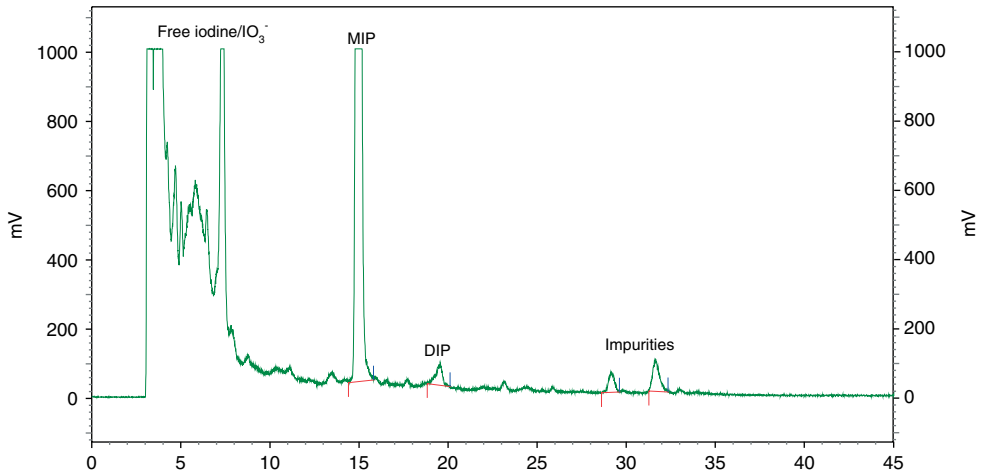

Figure 1. Radioactivity chromatogram demonstrating the radio-iodination of DAMGO. The first 10 min, free iodine is eluting, at 15 min the mono-iodinated peptide is eluting (MIP), followed by di-iodinated peptide (DIP) at 19 min.

we were interested in the BBB transport, the difference between the radioactivity measured in brain and background tissue was calculated and plotted *versus* time. Therefore, the mean radioactivity differences were first calculated per animal over 60 and 180 min scan time, respectively. Then, the animals injected with the same peptide were combined and the importance weighed for the injected dose. Finally, the mean differences between brain and background for the scans up to 60 and 180 min were combined.

Results

Quantitative Multi-criteria Evaluation: Desirability Function

The individual desirability values of each peptide as well as the global desirability value are listed in Table 3, where the peptides are already ranked from highest to lowest desirability. The combination of the four different biological parameters (K_{in}, k_{out}, $\log(k_{brain})$ and $\log(k_{plasma})$) into a global D-value revealed four groups:

1. High BBB-drugability: dermorphin
2. Reasonable BBB-drugability: DAMGO, TAPP, CTOP, TAPS
3. Low BBB-drugability: EM-1 and EM-2
4. No BBB-drugability: CTAP

The highest D-value, thus the highest drugability, was demonstrated for dermorphin, whereas CTAP did not show any drugability due to the fact that no influx occurred.

In order to make the initial kinetic constants more consistent in a comparable way, we recalculated the transfer constants, using only and exactly the first 10 min for each of the peptides. The same general conclusions were obtained compared to the previous data. Moreover, weighing of the four responses revealed more or less the same ranking for the first 10 min (see Supporting Information).

In vivo Imaging

Before starting the SPECT analysis, peptides were radiolabeled with I-123 and the mono-iodinated fraction was collected by HPLC. A typical chromatogram of this radio-iodination is illustrated for DAMGO in Figure 1. The radioactivity curve obtained for dermorphin after correction for the injected dose is shown in Figure 2. This figure demonstrates that the radioactivity reaching the brain is only slightly higher compared to the background. The curves, representing the radioactivity difference between brain and background tissue, are displayed in Figure 3. Finally, the mean differences between brain and background tissue for the scans up to 60 and 180 min are listed in Table 4. The data of the initial time frames (i.e. 10 × 1 min) were first combined into two groups, each 5 min, to obtain equal time frames. Then, the obtained SPECT counts in brain and background ROI were divided by the injected dose, followed by background correction. Next, the mean difference between brain and background was calculated over time. The injected dose was weighed over two mice and finally, the mean difference over two mice was calculated. Detailed information on this calculation is given in Supporting Information.

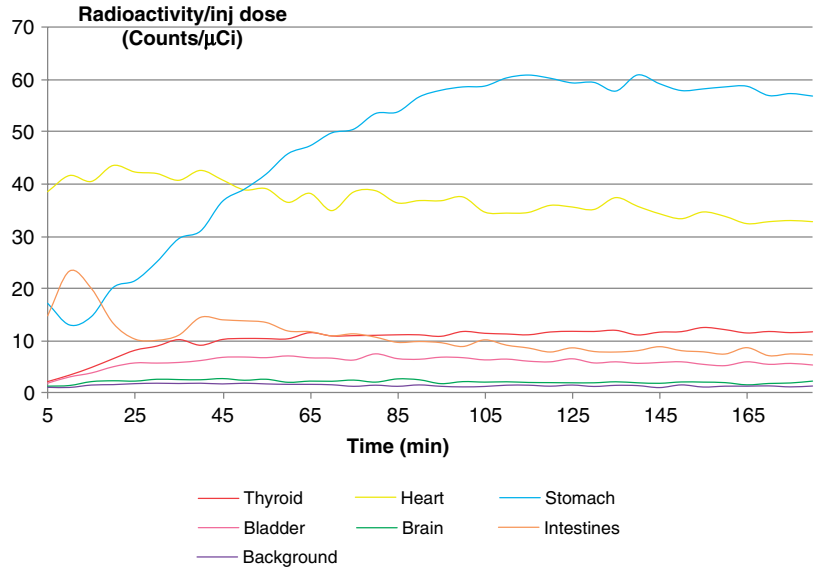

Figure 2. Radioactivity curve of dermorphin obtained after SPECT analysis for 3 h, corrected for the injected dose.

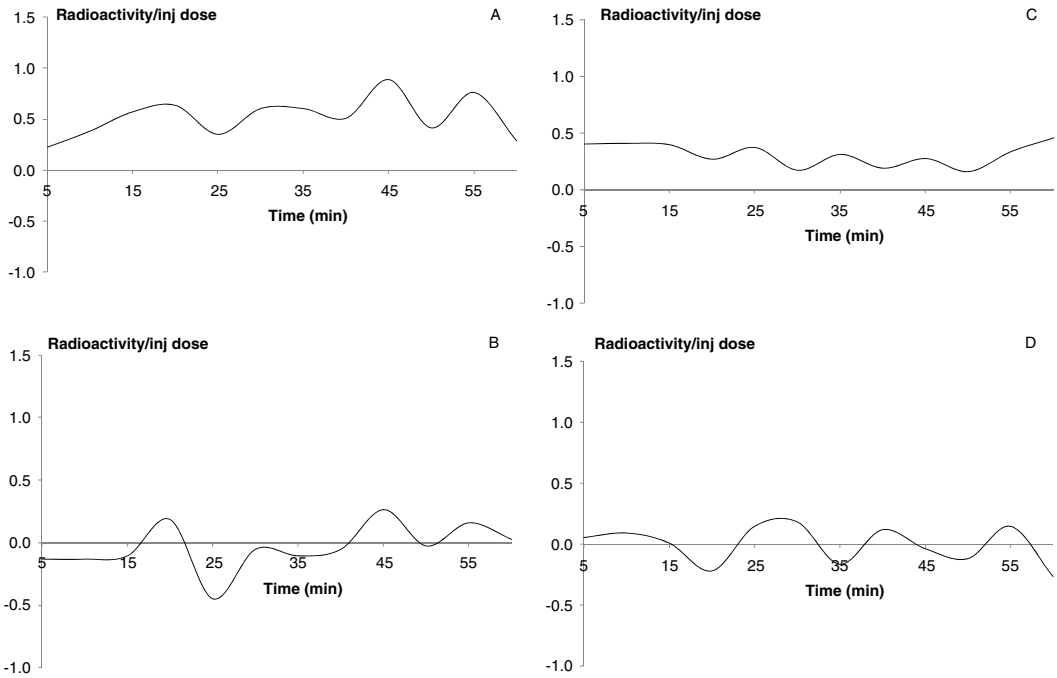

Figure 3. Radioactivity curves representing the brain-background difference over time. (A) Dermorphin, (B) EM-1, (C) DAMGO and (D) TAPP.

It is clearly demonstrated that two peptides (dermorphin and DAMGO) are able to enter the brain and thus penetrate the BBB, whereas the other peptides could not reach the brain at all. The background values were obtained the same way as the other values, with the ROI arbitrarily defined as the leg muscle, in which only low radioactivity was accumulated.

Discussion

Although peptides were long considered to be useless drug candidates due to their low drugability (e.g. chemical and metabolic instabilities), recent technological advancements have made them valuable and unique drug candidates. In order to reach brain receptors, such as MOR which are targeted in pain treatment, the peptides need to cross the BBB. Currently, there is great interest in developing more stable opioid peptides to improve BBB transport and metabolic stability [37–40].

In order to select the best peptide drug candidate, showing a high metabolic stability in plasma and brain, as well as a high influx penetration rate through the BBB combined with a low efflux rate, these different biological parameters were evaluated using a multi-criteria decision method. Moreover, due to the scaling differences of the selected parameters (K_{in}, k_{out}, log(k_{brain}) and log(k_{plasma})), such a comprehensive multi-criteria method is required. The highest global desirability value represents the peptide with the highest drugability. When taking into account

Journal of PeptideScience

Table 4. Weighed mean difference $\bar{\varepsilon}$ between brain and background calculated from the *in vivo* imaging analysis after 60 and 180 min

	Weighed mean $\bar{\varepsilon}$ (counts/μCi)	
Peptide	60 min	180 min
^{123}I-Dermorphin	0.19 ± 0.15	0.30 ± 0.17
^{123}I-EM-1	-0.07 ± 0.15	-0.07 ± 0.10
^{123}I-DAMGO	0.17 ± 0.09	0.13 ± 0.05
^{123}I-TAPP	-0.005	0.006

the influx and efflux at the BBB and the *in vitro* stability in mouse plasma and brain homogenate, the application of the desirability function to the eight opioid peptides revealed four groups:

1. High BBB-drugability: dermorphin
2. Reasonable BBB-drugability: DAMGO, TAPP, CTOP, TAPS
3. Low BBB-drugability: EM-1 and EM-2
4. No BBB-drugability: CTAP

Thus, dermorphin is shown to be the best BBB-penetrating peptide and the most stable in plasma and brain, whereas CTAP did not show any drugability at all. Although frequently applied in chromatography, this desirability (D) approach was never used in biomedical research, even though this approach can objectively reveal the best peptide drug candidate.

Additionally, the *in vivo* dynamic planar imaging in mice of four opioid peptides (EM-1, DAMGO, dermorphin and TAPP) upon intravenous injection of the I-123 peptide tracers was investigated in order to validate the above obtained desirability function. This *in vivo* analysis clearly confirmed that dermorphin is the best BBB-penetrating peptide with the highest metabolic stability in plasma and brain, followed by DAMGO. Thus, this peptide was selected as the best peptide drug candidate among the eight tested opioid peptides.

Although the radioactivity reaching the brain tissue is only slightly higher than that of the background in absolute terms, for dermorphin and DAMGO the difference between brain and background was clearly demonstrated and statistically significant. The other two peptides, EM-1 and TAPP, did not reveal any influx into the brain during the SPECT analysis. Comparing these *in vivo* imaging results with the obtained desirability of the peptides, it is obvious that dermorphin still represents the best BBB-penetrating peptide. Thus, the *in vivo* imaging results confirm and validate the multi-criteria approach.

Conclusion

A multi-criteria approach was applied to select the peptide with the highest BBB-drugability. Owing to the scaling differences of the selected BBB transport and metabolic stability parameters and their opposing characteristics, a multi-criteria method was required. The desirability function is used to simultaneously optimize the different parameters and objectively rank the peptides based on the quantitative desirability value. The results obtained with the desirability function were validated by *in vivo* SPECT imaging.

As a general conclusion, application of the desirability multi-criteria approach is promising in biomedical research, where it is often required to combine the different biological responses having a different scaling. This way it is possible to quantitatively and objectively select the best candidate.

Acknowledgements

This research was funded by PhD grants of 'Institute for the Promotion of Innovation through Science and Technology in Flanders (IWT-Vlaanderen)' (No. 73402) and 'Special Research Fund from the Ghent University (BOF)' (No. 01J06109).

Supporting information

Supporting information may be found in the online version of this article.

References

1. Spisani S, Fraulini A, Varani K, Falzarano S, Cavicchioni G. New chemotactic dimeric peptides show high affinity and potency at the human formylpeptide receptor. *Eur. J. Pharmacol.* 2007; **567**: 171–176.
2. Manning M, Cheng LL, Stoev S, Wo NC, Chan WY, Szeto HH, Durroux T, Mouillac B, Barberis C. Design of peptide oxytocin antagonists with strikingly higher affinities and selectivities for the human oxytocin receptor than atosiban. *J. Pept. Sci.* 2005; **11**: 593–608.
3. Igarashi H, Ito T, Mantey SA, Pradhan TK, Hou W, Coy DH, Jensen RT. Development of simplified vasoactive intestinal peptide analogs with receptor selectivity and stability for human vasoactive intestinal peptide/pituitary adenylate cyclase-activating polypeptide receptors. *J. Pharmacol. Exp. Ther.* 2005; **315**: 370–381.
4. Thomasy SM, Moeller BC, Stanley SD. Comparison of opioid receptor binding in horse, guinea pig, and rat cerebral cortex and cerebellum. *Vet. Anaesth. Analg.* 2007; **34**: 351–358.
5. Nepomuceno D, Sutton S, Yu J, Zhu J, Liu C, Lovenberg T, Bonaventure P. Mutagenesis studies of neuropeptide S identify a suitable peptide tracer for neuropeptide S receptor binding studies and peptides selectively activating the I107 variant of human neuropeptide S receptor. *Eur. J. Pharmacol.* 2010; **635**: 27–33.
6. Spetea M, Ötvös F, Tóth G, Nguyen TMD, Schiller PW, Vogel Z, Borsodi A. Interaction of agonist peptide [3H]Tyr-Ala-Phe-Phe-NH2 with [mu]-opioid receptor in rat brain and CHO-[mu]/1 cell line. *Peptides* 1998; **19**: 1091–1098.
7. Vonhof S, Barone FC, Price WJ, Paakkari P, Millison JH, Feuerstein GZ, Siren ALK. Receptor binding and biological activity of the dermorphin analog Tyr-D-Arg(2)-Phe-Sar (TAPS). *Eur. J. Pharmacol.* 2001; **416**: 83–93.
8. Medzihradszky K. The chemistry of the opioid receptor binding sites. *J. Pept. Sci.* 2003; **9**: 333–353.
9. Bickel U, Yoshikawa T, Pardridge WM. Delivery of peptides and proteins through the blood–brain barrier. *Adv. Drug Delivery Rev.* 2001; **46**: 247–279.
10. Egleton RD, Abbruscato TJ, Thomas SA, Davis TP. Transport of opioid peptides into the central nervous system. *J. Pharm. Sci.* 1998; **87**: 1433–1439.
11. Gao B, Hagenbuch B, Kullak-Ublick GA, Benke D, Aguzzi A, Meier PJ. Organic anion-transporting polypeptides mediate transport of opioid peptides across blood–brain barrier. *J. Pharmacol. Exp. Ther.* 2000; **294**: 73–79.
12. Prokai L. Peptide delivery into the central nervous system: Invasive, physiological and chemical approaches. *Expert Opin. Ther. Pat.* 1997; **7**: 233–245.
13. Abbott NJ, Patabendige AAK, Dolman DEM, Yusof SR, Begley DJ. Structure and function of the blood–brain barrier. *Neurobiol. Dis.* 2010; **37**: 13–25.
14. Kniesel U, Wolburg H. Tight junctions of the blood–brain barrier. *Cell. Mol. Neurobiol.* 2000; **20**: 57–76.
15. Pan WH, Tu H, Kastin AJ. Differential BBB interactions of three ingestive peptides: obestatin, ghrelin, and adiponectin. *Peptides* 2006; **27**: 911–916.
16. Banks WA, Kastin AJ, Coy DH. Evidence that [125I]N-Tyr-delta sleep-inducing peptide crosses the blood–brain barrier by a non-competitive mechanism. *Brain Res.* 1984; **301**: 201–207.

17. Weiner RE, Thakur ML. Radiolabeled peptides in the diagnosis and therapy of oncological diseases. *Appl. Radiat. Isot.* 2002; **57**: 749–763.
18. Keresztes A, Toth G, Fulop F, Szucs M. Synthesis, radiolabeling and receptor binding of [H-3][(1S,2R)ACPC(2)]endomorphin-2. *Peptides* 2006; **27**: 3315–3321.
19. Lien S, Lowman HB. Therapeutic peptides. *Trends Biotechnol.* 2003; **21**: 556–562.
20. Hau VS, Huber JD, Campos CR, Lipkowski AW, Misicka A, Davis TP. Effect of guanidino modification and proline substitution on the in vitro stability and blood–brain barrier permeability of endomorphin II. *J. Pharm. Sci.* 2002; **91**: 2140–2149.
21. Dangoor D, Biondi B, Gobbo M, Vachutinski Y, Fridkin M, Gozes I, Rocchi R. Novel glycosylated VIP analogs: synthesis, biological activity, and metabolic stability. *J. Pept. Sci.* 2008; **14**: 321–328.
22. Krondahl E, von Euler-Chelpin H, Orzechowski A, Ekström G, Lennernäs H. In vitro metabolism of opioid tetrapeptide agonists in various tissues and subcellular fractions from rats. *Peptides* 2001; **22**: 613–621.
23. Gentilucci L. New trends in the development of opioid peptide analogues as advanced remedies for pain relief. *Curr. Top. Med. Chem.* 2004; **4**: 19–38.
24. Biondi L, Filira F, Giannini E, Gobbo M, Lattanzi R, Negri L, Rocchi R. Novel glycosylated (LyS(7))-dermorphin analogues: synthesis, biological activity and conformational investigations. *J. Pept. Sci.* 2007; **13**: 179–189.
25. Izdebski J, Kunce D, Schiller PW, Chung NN, Gers T, Zelman M, Grabek M. Synthesis and biological activity of homoarginine-containing opioid peptides. *J. Pept. Sci.* 2007; **13**: 27–30.
26. Mosnaim AD, Puente J, Tse R, Wolf ME. In vitro human brain methionine-enkephalin metabolism. *FASEB J.* 2005; **19**: A509–A509.
27. Vergote V, Van Dorpe S, Peremans K, Burvenich C, De Spiegeleer B. In vitro metabolic stability of obestatin: kinetics and identification of cleavage products. *Peptides* 2008; **29**: 1740–1748.
28. Van Dorpe S, Adriaens A, Polis I, Peremans K, Van Bocxlaer J, De Spiegeleer B. Analytical characterization and comparison of the blood–brain barrier permeability of eight opioid peptides. *Peptides* 2010; **31**: 1390–1399.
29. Deming SN. Multiple-criteria optimization. *J. Chromatogr.* 1991; **550**: 15–25.
30. Derringer G, Suich R. Simultaneous-optimization of several response variables. *J. Qual. Technol.* 1980; **12**: 214–219.
31. Van Dorpe S, Vergote V, Pezeshki A, Burvenich C, Peremans K, De Spiegeleer B. Hydrophilic interaction LC of peptides: columns comparison and clustering. *J. Sep. Sci.* 2010; **33**: 728–739.
32. Ekins S, Honeycutt JD, Metz JT. Evolving molecules using multi-objective optimization: applying to ADME/Tox. *Drug Discov. Today* 2010; **15**: 451–460.
33. De Spiegeleer B, Vergote V, Pezeshki A, Peremans K, Burvenich C. Impurity profiling quality control testing of synthetic peptides using liquid chromatography-photodiode array-fluorescence and liquid chromatography-electrospray ionization-mass spectrometry: the obestatin case. *Anal. Biochem.* 2008; **376**: 229–234.
34. Chen WD, Lee W, Mulliss CL. On the rounding rules for logarithmic and exponential operations. *Chin. J. Phys.* 2005; **43**: 1017–1034.
35. Safa F, Hadjmohammadi MR. Simultaneous optimization of the resolution and analysis time in micellar liquid chromatography of phenyl thiohydantoin amino acids using Derringer's desirability function. *J. Chromatogr., A* 2005; **1078**: 42–50.
36. Derringer GC. A balancing act – optimizing a product's properties. *Qual. Prog.* 1994; **27**: 51–58.
37. Aldrich JV, Patkar KA, McLaughlin JP. Zyklophin, a systemically active selective kappa opioid receptor peptide antagonist with short duration of action. *Proc. Natl. Acad. Sci. U.S.A.* 2009; **106**: 18396–18401.
38. Fichna J, Do-Rego JC, Chung NN, Costentin J, Schiller PW, Janecka A. [Dmt(1), D-1-Nal(3)]morphiceptin, a novel opioid peptide analog with high analgesic activity. *Peptides* 2008; **29**: 633–638.
39. Janecka A, Perlikowska R, Gach K, Wyrebska A, Fichna J. Development of opioid peptide analogs for pain relief. *Curr. Pharm. Des.* 2010; **16**: 1126–1135.
40. Lukowiak M, Kosson P, Hennink WE, Lipikowski AW. Synthesis and pharmacological properties of a new fluorescent opioid peptide analog. *Pharmacol. Rep.* 2009; **61**: 727–731.

